Journal of Hydrology: Regional Studies 59 (2025) 102389

Contents lists available at ScienceDirect

Journal of Hydrology: Regional Studies

journal homepage: www.elsevier.com/locate/ejrh

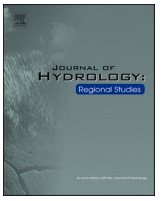

Impact of Tropical Cyclone on Coastal Phytoplankton Blooms and Underlying Mechanisms

Haiyi Shi [a,d,e,1], Ying Chen [a,d,e,1], Hui Zhao [a,c,d,e,*], Robert Mortimer [b], Gang Pan [a,b,d,f,*]

[a] College of Chemistry and Environmental Science, Guangdong Ocean University, Zhanjiang, China
[b] School of Humanities, York St John University, York, UK
[c] Southern Marine Science and Engineering Guangdong Laboratory (Zhuhai), Zhuhai, China
[d] Research Center for Coastal Environmental Protection and Ecological Resilience, Guangdong Ocean University, Zhanjiang, China
[e] Cooperative Research Center for Nearshore Marine Environmental Change, Guangdong Ocean University, Zhanjiang, China
[f] Jiangsu Jiuguan Institute of Environment and Resources, Yixing, China

ARTICLE INFO

Keywords:
Tropical cyclone
Buoy observation
Turbidity
Lagging correlation

ABSTRACT

Study Region: Northern Beibu Gulf, China
Study Focus: This study examines the impact of tropical cyclone (TC) "Wipha" (2019) on phytoplankton chlorophyll-*a* (Chl-*a*) dynamics, using observations from two buoy stations (S1 and S2). Results indicate that persistently high turbidity at the inner bay (station S1) restricted underwater light availability, resulting in an insignificant change in mean daily Chl-*a* concentrations, despite sufficient nutrients. Conversely, at the outer bay (station S2), Chl-*a* significantly increased after the storm, exhibiting notable delayed correlations with elevated turbidity ($r = 0.87$, $p < 0.01$) and aerosol deposition ($r = 0.90$, $p < 0.01$). The differential phenomenon at two locations highlights that distinct environmental control the responses of phytoplankton dynamics to the tropical cyclone, primarily related to light availability and nutrient sources.
New Hydrological Insights for the Region: In contrast to prior studies, the nutrient source leading to increased Chl-*a* at the outer bay may result from wet deposition of aerosols and re-suspension of suspended matter, rather than direct terrestrial nutrient inputs. Additionally, the prolonged turbidity recovery period (up to 5 days) at the inner bay substantially limited phytoplankton growth, highlighting TC-induced turbidity as a critical factor constraining phytoplankton blooms in eutrophic coastal environments.

1. Introduction

With global warming, the intensity and frequency of tropical cyclones is significantly increasing in recent years (Li et al., 2023; Wang et al., 2022). Tropical cyclones are among the most devastating natural disasters. They significantly impact coastal regions due to their high destructiveness and frequent occurrences (Wang and Toumi, 2021). Coastal seas are critical interfaces between lands and oceans. Rapid socioeconomic development has introduced excessive terrigenous nutrients into coastal waters. This has caused severe

* Corresponding authors at: College of Chemistry and Environmental Science, Guangdong Ocean University, Zhanjiang, China.
E-mail addresses: huizhao1978@163.com (H. Zhao), g.pan@yorksj.ac.uk (G. Pan).
[1] These authors share first authorship

https://doi.org/10.1016/j.ejrh.2025.102389
Received 2 January 2025; Received in revised form 30 March 2025; Accepted 11 April 2025
Available online 16 April 2025

coastal eutrophication and frequent phytoplankton blooms (Herbeck et al., 2011; Wang et al., 2021). Frequent tropical cyclones may further worsen these phenomena. Therefore, it is essential to understand how tropical cyclones influence coastal phytoplankton blooms.

In open sea areas, phytoplankton blooms mainly occur due to the upwelling and mixing of "new" nutrients from subsurface layer caused by strong winds of tropical cyclones (Chen et al., 2003; Lin, 2012). In coastal areas, the increase in phytoplankton is primarily due to the advection of nutrients from increased terrestrial runoff as well as entrainment of nutrients by strong mixing in shallow continental shelf regions (Zhao et al., 2017). When a typhoon passes through, the resulting changes in water temperature and salinity can significantly affect the phytoplankton community structure (Chen et al., 2004). Certain species may become dominant in the altered environmental conditions, causing shifts in the community composition. Furthermore, typhoon-induced rainfall introduces nutrients from land into the ocean via river runoff, which stimulates phytoplankton growth (Zheng and Tang, 2007). This increases nutrient levels in nearshore waters and promotes phytoplankton blooms. Tropical cyclone events in coastal areas can generally increase water turbidity due to the re-suspension of coastal sediments or terrestrial inputs with higher levels of nutrients (Thompson et al., 2023). Studies indicated a positive relationship existed often between turbidity values and Chlorophyll-*a* (Chl-*a*) in view of higher turbidity accompanied by higher nutrients input (Fragoso et al., 2024). However, on the other hand, high turbidity may trigger a decrease in water transparency, leading to light restriction for phytoplankton photosynthesis under the nutrients-rich conditions, which is unfavorable to phytoplankton growth and increase in chlorophyll (Babin et al., 2004; Rhee and Gotham, 1981). Understanding the recovery time of water column turbidity following tropical cyclones is essential for explaining the mechanisms behind coastal blooms. This knowledge will improve our understanding of how these disturbances impact the primary productivity of marine ecosystems.

The tropical cyclone (TC) "Wipha" was originated northwest of the central basin on July 31, 2019, moved northwestwards and passed through the north coastal region of Beibu Gulf during August 2–3 with the speeds over 20 m s^{-1}. This study aims to investigate the pattern of changes in Chl-*a* concentration at two stations during "Wipha" and reveal the key mechanisms behind phytoplankton changes induced by the TC at two buoy stations (S1 and S2). We will analyze data collected during TC in 2019, including Chl-*a*, turbidity, nutrients, and other environmental factors to understand the impact of cyclone on coastal ecosystems, providing insights for better prevention and management strategies.

2. Materials and methods

2.1. Data

2.1.1. Tropical cyclones data

The TC track data are accessible from the best-track typhoon dataset provided by Typhoon Online (www.typhoon.org.cn) (Lu et al., 2021; Ying et al., 2014). The data includes the Maximum Sustained Wind (MSW) and the longitude/latitude coordinates of the typhoon's center every 3 hours. In this paper, we selected Wipha in summer of 2019 as the research object. The responses of hydrological and water quality parameters to TC were analyzed before TC (July 26–31), during TC (August 1–4) and after TC (August 5–16).

2.1.2. Satellite and Modeling products

6-hourly Advanced Scatterometer (ASCAT) sea surface wind (SSW) data, provided by the Remote Sensing System (www.remss.com/), were utilized in the study at a spatial resolution of 0.25°× 0.25°. Daily precipitation data from the Tropical Rainfall Measuring Mission (TRMM) of the National Aeronautics and Space Administration (NASA) (https://gpm.nasa.gov/data) were

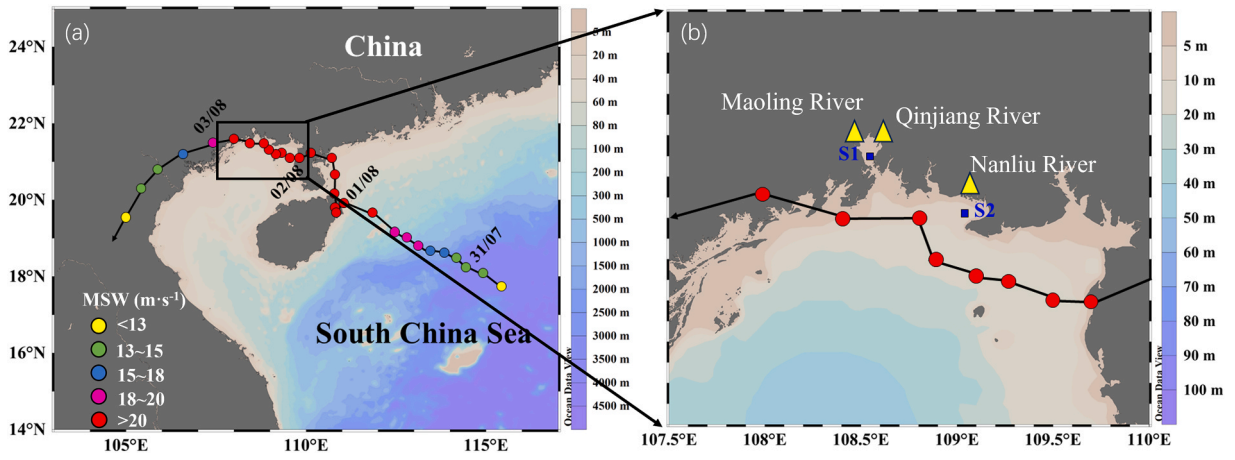

Fig. 1. (a) Track and intensity of TC "Wipha" in the northwestern South China Sea. Dates are given as dd/mm. MSW: maximum sustained wind speed. (b) Depth map of the northern Beibu Gulf in the study area (black box in Fig. 1a) (20.5° N - 22.5° N, 107.5° E - 110° E). Yellow triangles mark the river estuaries. Blue squares are the buoy-based fixed-point observational stations (S1 and S2).

obtained at a spatial resolution of 0.10°× 0.10°.

This study used long-term global dust deposition (DEP) reanalysis data from NASA's Global Modelling and Assimilation Office (GMAO) (https://disc.gsfc.nasa.gov/datasets/) were also used in this study. The dataset includes extended assimilated aerosol information, such as dry and wet deposition of aerosol components, dust emission and sedimentation for each size bin, and organic carbon convective scavenging. It has a spatial resolution of 0.5°× 0.625°. The hourly dust dry and wet deposition from 'Bin 001' to 'Bin 005' in MERRA-2 were accumulated to evaluate daily DEP over the study area during TC.

2.1.3. In situ observations

Two buoys with water quality sensors were deployed at stations S1 and S2 in the northern Beibu Gulf (Fig. 1). At a depth of 0.5 m below the sea surface, continuous measurements of temperature, salinity, pH, dissolved oxygen (DO), turbidity, and Chl-*a* were taken using a YSI 6600V2 multiparameter water quality instrument (YSI Inc., Yellow Springs, USA), with data collected every thirty minutes. A Systea nutrient probe analyzer (NPA; Systea S.p.A., Anagni, Italy) was used to detect dissolved inorganic nitrogen (DIN) and phosphorus (P) every four hours. After all observations were completed, invalid or missing data were interpolated linearly to produce a complete time series.

2.2. Methods

2.2.1. Lagged correlation

The lagged correlation quantifies the similarity between two time series, considering potential time lags. By calculating correlations at different time lags, it can identify when the similarity between the two series is strongest. The purpose of lagged correlation is to address the limitations of traditional correlation analysis, which cannot capture the lagged relationships in time series data (Na et al., 2021).

Firstly, two time series datasets were adjusted to the same length and ensured to have identical time intervals. Secondly, for each possible time lag value (ranging from 0 to 7 days), the correlation coefficient between two series was calculated, respectively. For instance, for a lag value of k, the correlation coefficient between series A (environmental factor) and series B (Chl-*a*) at lag k was computed :

$$Corr_k = \frac{\sum_{t=1}^{N-k}(A_t - \overline{A})(B_{t+k} - \overline{B})}{\sqrt{\sum_{t=1}^{N-k}(A_t - \overline{A})^2}\sqrt{\sum_{t=1}^{N-k}(B_{t+k} - \overline{B})^2}} \quad (1)$$

where N is the total number of observations in the time series, t is time index, A_t is observed value of variable A at time t, B_{t+k} is observed value of variable B at time $t + k$, $\overline{A}$ and $\overline{B}$ are average of variable A and B.

Finally, among all calculated lagged correlation coefficients, the lag value corresponding to the maximum absolute correlation coefficient was selected as the optimal lag. In this study, we conducted lag correlation analyses between Chl-*a* and environmental factors (temperature, salinity, pH, DO, turbidity, DIN, P, SSW, precipitation and DEP) for lag values from 0 to 7 days.

3. Results

3.1. Precipitation and SSW

Before the TC arrived in the study area, S1 and S2 experienced rainfall starting on July 27, which continued throughout the TC period (Fig. 2). The maximum daily precipitation of nearly 80 mm at S2 occurred on July 28. In contrast, the daily precipitation at

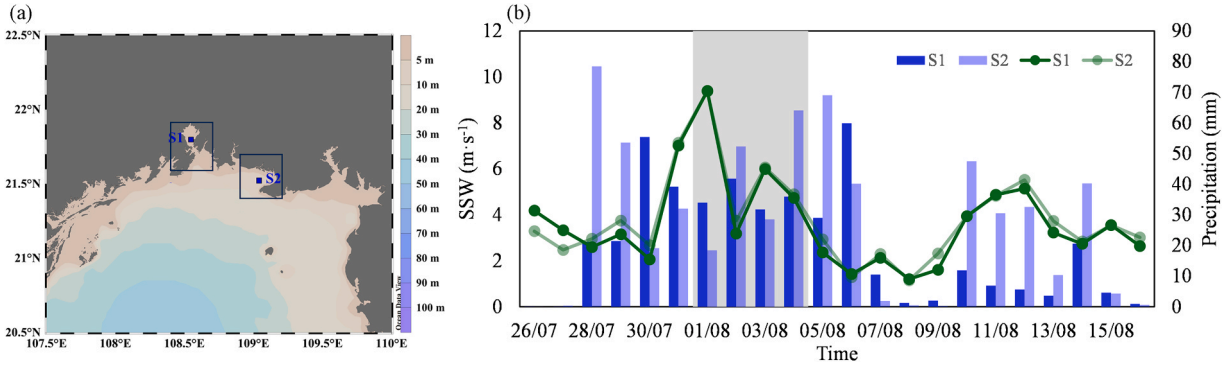

Fig. 2. Regional range (a) of daily values for precipitation and SSW (black boxes). Time series (b) of precipitation (mm) (blue bar) and SSW (m s^{-1}) (green line) in S1 and S2 from July 26 to August 16, 2019. Gray shading indicates the periods of TC occurrence (i.e., stations S1 and S2 within the typhoon influence radius).

station S1 was below 60 mm. Higher SSW began to increase from July 30. Wind speed trends at both stations were generally consistent. The maximum mean wind speed reached approximately 10 m s^{-1} on August 1 (Fig. 2).

3.2. The hydrological and biochemical factors in the inner bay area

S1 is in an inner bay significantly affected by land-based sources, with two rivers flowing into it (Fig. 1b). When the TC arrived, the temperature dropped sharply from July 31, reaching its lowest value of 26.61 °C on August 4, about 5 °C lower than on July 30 (before TC). The temperature at S1 took about 8 days to return to the pre-typhoon levels of ~31 °C from August 4 (Fig. 3). Due to its location, the initial salinity at S1 was low (~10) before the TC. Salinity began to decrease on August 2, with its lowest value of about 2 on August 4. It took approximately 11 days from August 4 for the salinity at S1 to return to the pre-typhoon levels (Fig. 3). DO gradually increased on July 31, reaching a maximum of about 6.5 mg L^{-1} on August 3, with an increase of approximately 0.8 mg L^{-1}. After this peak, DO began to decrease on August 3, taking about 8 days to return to the pre-typhoon levels (Fig. 3). Tropical cyclones are usually accompanied by heavy rainfall, which can increase freshwater input into the bay. The influx of freshwater can dilute salinity and the concentration of dissolved substances, affecting pH. pH began to decrease on August 2, with the lowest value of about 7.05 on August 5, a decrease of about 0.7 from before the TC. pH began to rise on August 5, taking about 8 days to return to the pre-typhoon levels at S1 (Fig. 3). Affected by the input from two rivers, the turbidity changes were very significant. Turbidity began to increase on August 2, reaching 195 NTU on August 3, an increase of about 1850 % from before the TC. Turbidity began to decrease on August 4, and it took approximately 5 days for the S1 site to return to its pre-typhoon levels (Fig. 3). Significant variation of Chl-*a* levels at S1 was not observed before and after the TC, remaining around 4.5 mg m^{-3}. There was a brief small peak in Chl-*a* on August 4. However, the daily average concentration remained largely unchanged compared to the pre-typhoon levels. (Fig. 3). During TC, DIN concentration increased with P decreasing at the earlier stage (August 1–4) and then decreased with P increasing at the 2 stage (August 7–13) and P-limitation further being alleviated, suggesting that there are more nutrients can be utilized from 10 August. Before August 2 and after August 12, the DIN to P ratio at S1 was close to the optimal ratio of 16:1. However, as P concentration decreased, the area gradually shifted to P limitation from August 3 up to August 12. During TC, DIN increased by about 5.7 μmol L^{-1}, while P decreased by 0.66 μmol L^{-1}.

3.3. The hydrological and biochemical factors in the outer bay area

S2 is in the outer bay and is influenced by land-based sources, including one river. When the TC arrived, the temperature began to drop sharply from July 31, reaching its lowest point on August 3, at 27.45 °C, which was about 4 °C lower than before the TC. It took approximately 5 days for the temperature at S2 to return to the pre-typhoon levels after August 3 (Fig. 4). Salinity started to decrease on August 1, reaching a minimum of about 18 around August 4. After TC, salinity at S2 remained lower than before TC (Fig. 4). The variation in DO during the TC was not significant, but there was a peak after the TC. DO began to increase on August 6, reaching a maximum of about 10 mg L^{-1} on August 8, an increase of approximately 3 mg L^{-1}. It then decreased, returning to the pre-typhoon

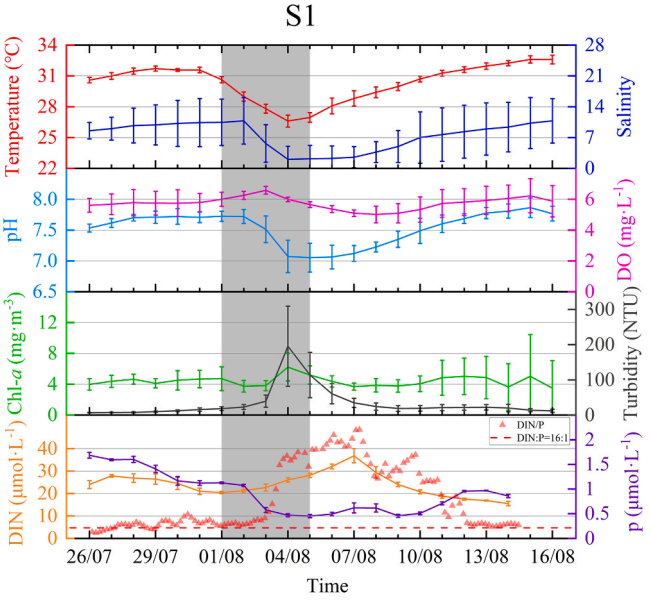

Fig. 3. Time series of temperature (℃), salinity, pH, DO (mg L^{-1}), Chl-*a* (mg m^{-3}), turbidity (NTU), DIN (μmol L^{-1}), and P (μmol L^{-1}) at S1 from July 26 to August 16, 2019. The polylines (bold lines) represent the daily average value and their corresponding standard error (error bar). Gray shading indicates periods of TC occurrence (i.e., station S1 within the typhoon influence radius).

levels after 2 days (Fig. 4). pH started to decrease on July 31, reaching a low of about 7.97 around August 4, which is a decrease of about 0.2 from before the TC. It began to rise on August 4, returning to pre-typhoon levels about 4 days later before decreasing again (Fig. 4). Affected by the input from one river, the turbidity changes caused by the TC were also quite significant. Turbidity began to increase on July 31, peaking at 120 NTU on August 2, which is an increase of about 100 NTU from before TC. Turbidity started to decrease on August 2, returning to the pre-typhoon levels at S2 in about 3 days (Fig. 4). Chl-*a* increased significantly after TC, showing a delayed response. It started to rise on August 5, exceeding 15 on August 7 and 8. After August 8, Chl-*a* levels began to decline, returning to the pre-typhoon levels by August 10 (Fig. 4). During the TC, both DIN and P concentrations increased. At S2, the DIN ratio was close to the optimal 16:1 during the TC. DIN increased by approximately 14 μmol L^{-1}, while P increased by 1.43 μmol L^{-1} during the TC (Fig. 4).

3.4. Changes in turbidity and Chl-a caused by TC

Before the TC, the average Chl-*a* concentration at S1 was 4.39 mg m^{-3}. After the TC, Chl-*a* levels remained stable at an average of 4.33 mg m^{-3}, only a change of −1.5 % from before TC. TC caused a 19-fold increase in turbidity with a recovery time of 5 days (Table 1). Before the TC, the average Chl-*a* concentration at S2 was 5.41 mg m^{-3}. After the TC, Chl-*a* peaked at an average of 8.92 mg m^{-3}, with an increase of 42.51 % from before TC. While TC caused a 10-fold increase in turbidity with a recovery time of 3 days (Table 1).

3.5. Lagged Correlation Analysis

Fig. 5 shows the lagged correlation between Chl-*a* and various environmental factors. Analyzing the impact of environmental factors with different time lags on Chl-*a* concentration reveals potential causal relationships and lag effects. Chl-*a* concentration at S1 is significantly positively correlated with turbidity ($r = 0.68$, $p < 0.05$). At lag 1 day, Chl-*a* concentration at S1 is significantly positively correlated with DO ($r = 0.49$, $p < 0.05$).At lag 4 days, the Chl-*a* concentration at S2 shows a strong negative correlation with SST ($r = -0.62$, $p < 0.05$). At S2, Chl-*a* showed a significant positive correlation with both pH and DO ($r = 0.54$, $p < 0.05$ and $r = 0.92$, $p < 0.01$). Both pH and DO react immediately to changes in Chl-*a*. At lag 5 days, Chl-*a* concentration shows a significant positive correlation with TUR ($r = 0.87$, $p < 0.01$). At lag 3 days, Chl-*a* concentration shows a significant positive correlation with PRE ($r = 0.68$, $p < 0.05$). Notably, a significant lag correlation exists between Chl-*a* and DEP in both areas. Specifically, at S1, there is a positive correlation with a lag of 2 days ($r = 0.63$, $p < 0.05$). At S2, the positive correlation occurs with a lag of 5 days ($r = 0.90$, $p < 0.01$).

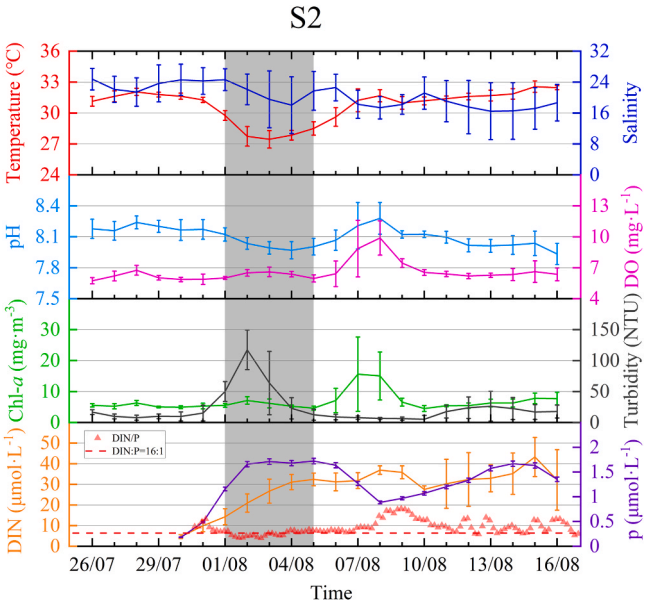

Fig. 4. Time series of temperature (℃), salinity, pH, DO (mg L^{-1}), Chl-*a* (mg m^{-3}), turbidity (NTU), DIN (μmol L^{-1}), and P (μmol L^{-1}) at S2 from July 26 to August 16, 2019. The polylines (bold lines) represent the daily average value and the corresponding standard error (error bar). Gray shading indicates periods of TC occurrence (i.e., station S2 within the typhoon influence radius).

Table 1
The Chl-*a* (mg m^{-3}) changes caused by TC at S1 and S2 before (July 26–31) and after (August 5–16) TC. The turbidity (NTU) changes caused by TC and the turbidity recovery time at S1 and S2. It should be noted that the turbidity changes caused by TC are from August 4–9 at S1, and from August 2–5 at S2.

	Chl-*a* (mg m^{-3})			Turbidity (NTU)	
	Before TC	After TC	▲Chl-*a*	Turbidity changes caused by TC	Turbidity recovery time
S1	4.39	4.33	−1.5 %	101.27	5 days
S2	5.41	7.71	+ 42.51 %	63.64	3 days

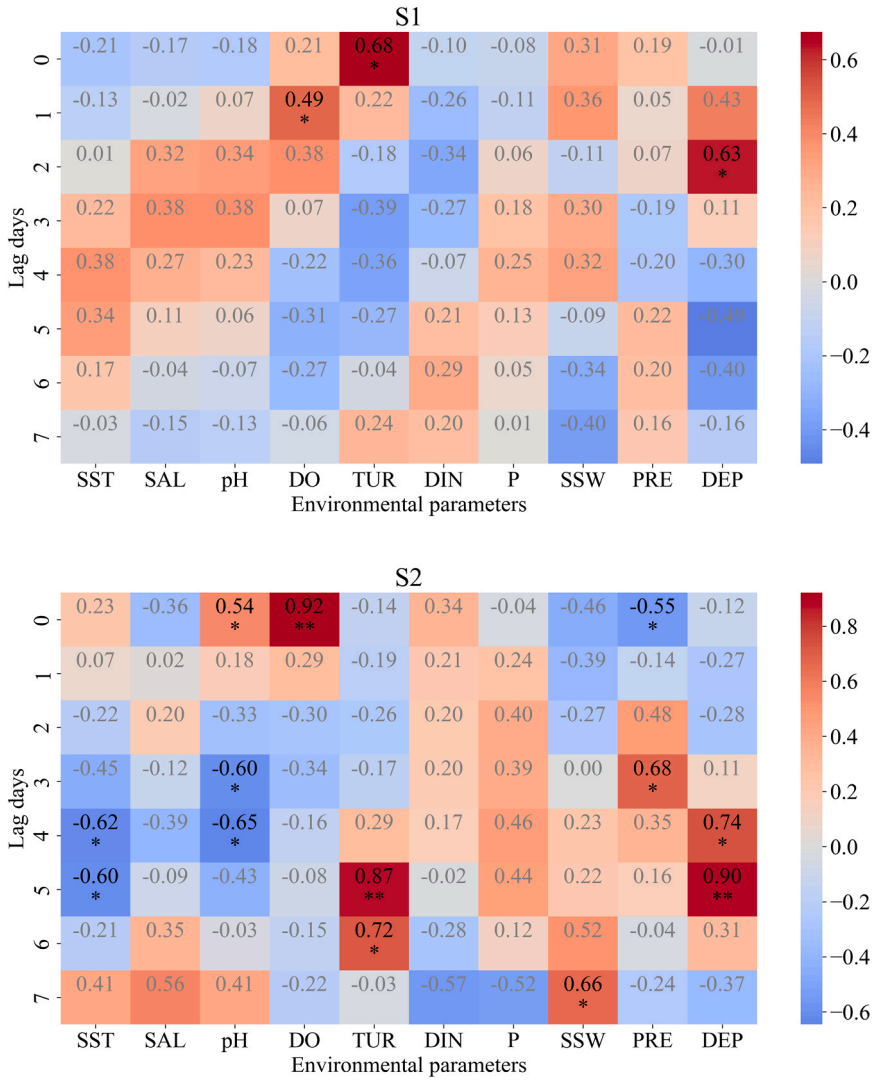

Fig. 5. Lagged correlation analysis of daily average Chl-*a* and environmental factors at S1 and S2 (sea surface temperature: SST; salinity: SAL; dissolved oxygen: DO; turbidity: TUR; dissolved inorganic nitrogen: DIN; phosphorus: P; sea surface wind: SSW; precipitation: PRE; dust deposition: DEP). The numerical values in the grid boxes are correlation coefficients. The colorbar is the degree of correlation. The asterisk indicates significance (* $p < 0.05$; ** $p < 0.01$).

4. Discussion

4.1. Impact of turbidity recovery time on phytoplankton blooms

Strong mixing caused by tropical cyclones commonly brings nutrient-rich cold water to the surface, lowering sea surface temperatures, and promoting phytoplankton growth and blooms (Liu et al., 2020; Ye et al., 2013; Zhao and Wang, 2018). However, Chl-*a*

level did not present similar pattern at S1 in the inner bay during the TC (Table 1), compared with previous studies. This phenomenon is unusual. Only a small peak in Chl-*a* levels occurred on August 4, likely due to increasing terrestrial freshwater carrying high oxygen concentrations and high biomass inputs (Fig. 3) in view of the fact that there were generally higher phytoplankton concentrations and oxygen concentration in fresh water than sea water (Jackson et al., 1987; Nilsson and Randall, 2010). These above processes caused the elusive lagged correlations of Chl-*a* with DO as well as turbidity. Specifically, Chl-a showed a significant 1-day positive lagged correlation with DO ($r = 0.49$, $p < 0.05$) and a significant immediate positive lagged correlation with turbidity ($r = 0.68$, $p < 0.05$) suggested that high Chl-*a* from terrestrial input is accompanied by high turbidity. Higher turbidity in previous studies suggested that there is strong re-suspension of organic matter, which consumes a lot of Do (Garnier et al., 2008). In fact, this significant correlation is caused by high DO due to freshwater input and high turbidity due to high Chl-*a*, rather than an increase in DO from phytoplankton growth.

Tropical cyclone occurrences, characterized by heavy rainfall over short periods (Groisman et al., 1999) (Fig. 2), result in increased coastal runoff. Furthermore, typhoon-induced mixing can lead to the resuspension of underlying sediments (Thompson et al., 2023). These processes change hydrological patterns, material cycles, and significantly affect marine ecosystems and climate (Dhillon and Inamdar, 2013; Fraser et al., 2018; Lin et al., 2022). To intuitively examine the water exchange dynamics at station S1, we selected data from two monitoring points (A1 and A2, Fig. 6) along the pathway of water flow from the inner bay to the outer bay for auxiliary analysis. The monitoring parameters and specifications at these points are identical to those at stations S1 and S2. S1 is in an inner bay where two rivers converge, implying that during TC, river discharge may increase, bringing substantial amounts of freshwater and impurities. This creates strong salinity and temperature gradients in the bay (Fig. 6). The mixing of freshwater and seawater changes water density, triggering convection and influencing salinity and temperature distribution (Lao et al., 2023). Significant shifts in salinity and temperature gradients (Fig. 6) during the TC suggest intense mixing in estuarine waters, causing large turbidity changes (>100 NTU) (Fig. 3 and Table 1).

High concentrations of suspended matter significantly regulate the physical, chemical, and biological interactions between dissolved substances and particles (Gebhardt et al., 2005). Particle-attached bacteria dominate bacterial activity. High concentrations of suspended matter enhance bacterial mineralization of organic carbon, converting it into dissolved inorganic nutrients like nitrogen and phosphorus, which indirectly promote phytoplankton growth (Crump and Baross, 1996; Ploug et al., 2002; Servais and Garnier, 2006). High concentrations of suspended particles also reduce light penetration, limiting phytoplankton growth (Garnier et al., 2001). Therefore, after TC, the recovery time of water turbidity is crucial for light penetration and requires careful attention, which matches past study (Thompson et al., 2023). During TC, turbidity at S1 was high and took 5 days to recover. It was longer than the recovery time for S2 (Fig. 3 and Table 1). This implies that turbidity indirectly affects phytoplankton growth by reducing light, explaining the smaller changes in Chl-*a* levels before and after the TC compared to S2. The weak correlation between Chl-*a* and environmental factors at S1 highlights the importance of light availability in nearshore eutrophic areas.

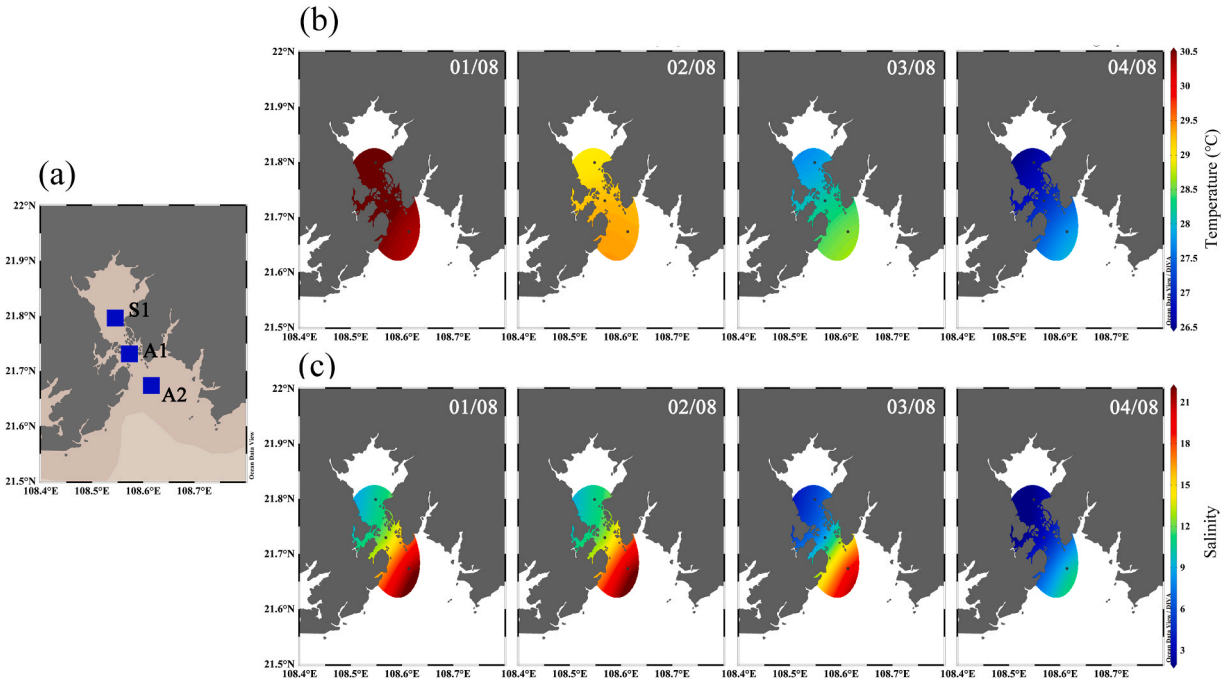

Fig. 6. (a) S1 and supplementary station for A1 and A2. (b) The temperature in S1, A1, and A2 during TC (01/08–04/08). (c) The salinity in S1, A1, and A2 during TC (01/08–04/08). Dates are given as dd/mm.

4.2. New insights into the mechanism of phytoplankton blooms caused by tropical cyclones

In the marine environment, the growth of Chl-*a* shows a delayed response to changes in environmental conditions (Gai et al., 2012). Previous studies have shown that there is a time lag (within a week) for strong surface winds to stimulate phytoplankton blooms (Brown and Ozretich, 2009; Gai et al., 2012). Our study found a clear lag between Chl-*a* and SSW during TC ($r = 0.66$, $p < 0.05$). Additionally, increased rainfall contributes more freshwater and runoff, which lowers SST. Chl-*a* was negatively correlated with SST, showing a delayed peak ($r = -0.62$, $p < 0.05$) 4 days later. Phytoplankton produce oxygen through photosynthesis, which directly raises DO levels of seawater and increases pH (Ling et al., 2017). At S2, similar results were observed, showing a significant positive correlation between Chl-*a*, DO, and pH (Chl-*a* vs DO: $r = 0.92$, $p < 0.01$; Chl-*a* vs pH: $r = 0.54$, $p < 0.05$).

Our results show several noteworthy phenomena. Ch-*a* showed a 3-day significant lagged positive correlation with precipitation ($r = 0.68$, $p < 0.05$). The primary reason may be that strong rainfall deposits aerosol-derived nutrients into the ocean, significantly increasing phytoplankton biomass (Yuan et al., 2023). Like other studies, typhoons cause more nitrogen wet deposition (Law et al., 2011; Tan et al., 2023). Aerosols typically enter the ocean through wet deposition following heavy rainfall, requiring several days to settle into the surface water and potentially affecting phytoplankton after 4–5 days (Yuan et al., 2023). This lag effect is particularly evident at station S2 (Fig. 5, $r = -0.90$, $p < 0.05$), suggesting that aerosol deposition could be one of the significant nutrient sources for phytoplankton growth in this area. Moreover, we observed no significant correlation between Chl-*a* and nutrients (DIN and P) at S2 (Fig. 5), which is not surprising in nutrient-rich coastal areas. However, DIN and TUR showed a strong correlation ($r = -0.68$, $p < 0.05$), while the correlation with DEP was weaker than with TUR ($r = -0.63$, $p < 0.05$). This suggests that nitrogen primarily originates from suspended matter. Weak correlations were found between P and both TUR and DEP (Fig. 7), suggesting that P may have widely sources. Chl-*a* had a significant 5-day lagged positive correlation with turbidity ($r = 0.87$, $p < 0.01$) and no significant lag correlation with salinity (Fig. 5), indicating that Chl-*a* in S2 was also influenced by nutrient release from suspended matter resuspension. Typhoon-induced water mixing and sediment disturbance raised turbidity (Huang et al., 2022; Thompson et al., 2023). Nutrients release from sediment promoted phytoplankton growth, but the response required some time. The turbidity increase is an immediate physical process, while phytoplankton growth is a delayed biological process, leading to an increase in Chl-*a* concentration after 5 days. Additionally, turbidity just began to recover after the 3th day (Table 1). Therefore, in addition to aerosol deposition, improved light conditions and nutrient release from resuspended matter also contributed to the phytoplankton blooms at S2.

5. Conclusion

The study offers new insights into the mechanisms driving phytoplankton blooms caused by TC, using TC "Wipha" in 2019 as a case study. Our findings highlighted the critical role of turbidity recovery time, sediment resuspension, and aerosol deposition in

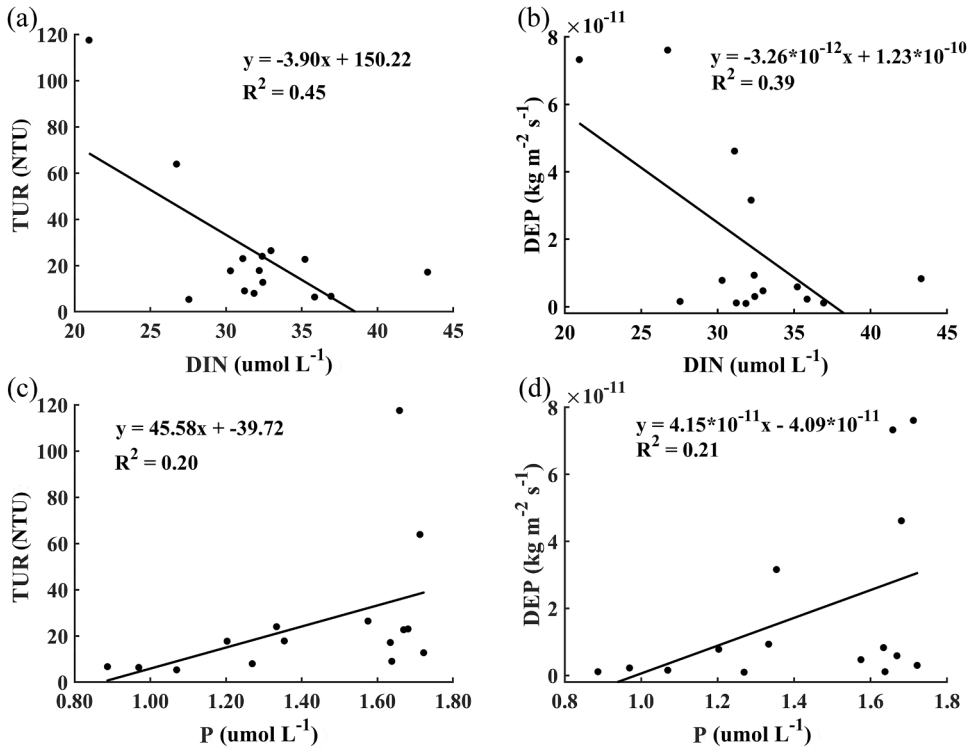

Fig. 7. Linear relationships between nutrients (DIN and P) and water quality parameters (turbidity and dust deposition).

controlling phytoplankton dynamics. Observations showed that turbidity levels at station S1 surged during TC and required up to 7 days to return to normal, demonstrating that increased turbidity reduces light availability and consequently constrains phytoplankton growth. The similar mean-daily Chl-*a* levels at station S1 before and after the TC suggested that light availability, rather than nutrient supply, was likely the primary limiting factor for phytoplankton growth. Moreover, lagged correlation analysis showed significantly positive correlations between Chl-*a* concentrations at station S2 and turbidity (5-day lag), dust deposition (5-day lag), and precipitation (3-day lag). These results indicated that elevated Chl-*a* levels at station S2 were primarily attributed to sediment resuspension and aerosol wet deposition, rather than direct terrestrial nutrient inputs.

Limitations of this study include its focus on a single storm event and the relatively short observational period surrounding the storm, which restricts the investigation of long-term ecological responses and phytoplankton community succession following the TC disturbances. Future research should extend both temporal and spatial coverage by incorporating multiple storm events across diverse coastal environments. Furthermore, integrating additional biological and chemical parameters, coupled with in situ sampling of aerosol nutrients, would provide deeper insights into nutrient pathways and phytoplankton responses.

Despite these limitations, our results underscore the importance of considering turbidity dynamics and aerosol nutrient inputs when assessing storm-induced ecological changes. These findings can be incorporated into models to improve predictions of phytoplankton blooms under changing climatic conditions.

Funding

The author(s) declared financial support was received for the research, authorship, and/or publication of this article. This study is supported by program for scientific research start-up funds of Guangdong Ocean University (No. 060302122304), National Natural Science Foundation of China (No. 42076162) and the project was supported by the Innovation Group Project of Southern Marine Science and Engineering Guangdong Laboratory (Zhuhai) (No. 311020004).

CRediT authorship contribution statement

Pan Gang: Writing – review & editing. **Mortimer Robert:** Writing – review & editing. **Zhao Hui:** Writing – review & editing, Supervision, Funding acquisition, Conceptualization. **Chen Ying:** Writing – review & editing, Visualization, Methodology, Data curation. **Shi Haiyi:** Writing – review & editing, Writing – original draft, Visualization, Methodology, Formal analysis, Data curation, Conceptualization.

Declaration of Competing Interest

The authors declare that they have no known competing financial interests or personal relationships that could have appeared to influence the work reported in this paper.

Data availability

Data will be made available on request.

References

Babin, S.M., Carton, J.A., Dickey, T.D., et al., 2004. Satellite evidence of hurricane-induced phytoplankton blooms in an oceanic desert. J. Geophys. Res.: Oceans 109. https://doi.org/10.1029/2003JC001938.

Brown, C.A., Ozretich, R.J., 2009. Coupling between the coastal ocean and yaquina bay, oregon: importance of oceanic inputs relative to other nitrogen sources. Estuar. Coast 32, 219–237. https://doi.org/10.1007/s12237-008-9128-6.

Chen, C.-T.A., Liu, C.-T., Chuang, W.S., et al., 2003. Enhanced buoyancy and hence upwelling of subsurface kuroshio waters after a typhoon in the southern east China sea. J. Mar. Syst. 42, 65–79. https://doi.org/10.1016/S0924-7963(03)00065-4.

Chen, Y.-L.L., Chen, H.-Y., Gong, G.-C., et al., 2004. Phytoplankton production during a summer coastal upwelling in the East China Sea. Cont. Shelf Res. 24, 1321–1338. https://doi.org/10.1016/j.csr.2004.04.002.

Crump, B., Baross, J., 1996. Particle-attached bacteria and heterotrophic plankton associated with the columbia river estuarine turbidity maxima. Mar. Ecol. Prog. Ser. 138, 265–273. https://doi.org/10.3354/meps138265.

Dhillon, G.S., Inamdar, S., 2013. Extreme storms and changes in particulate and dissolved organic carbon in runoff: entering uncharted waters? Geophys. Res. Lett. 40, 1322–1327. https://doi.org/10.1002/grl.50306.

Fragoso, G.M., Dallolio, A., Grant, S., et al., 2024. The role of rapid changes in weather on phytoplankton spring bloom dynamics from mid-norway using multiple observational platforms. J. Geophys. Res.: Oceans 129, e2023JC020415. https://doi.org/10.1029/2023JC020415.

Fraser, C.I., Morrison, A.K., Hogg, A.M., et al., 2018. Antarctica's ecological isolation will be broken by storm-driven dispersal and warming. Nat. Clim. Change 8, 704–708. https://doi.org/10.1038/s41558-018-0209-7.

Gai, S., Wang, H., Liu, G., et al., 2012. Chlorophyll a increase induced by surface winds in the northern south China sea. Acta Oceanol. Sin. 31, 76–88. https://doi.org/10.1007/s13131-012-0222-z.

Garnier, J., Servais, P., Billen, G., et al., 2001. Lower seine river and estuary (france) carbon and oxygen budgets during low flow. Estuaries 24, 964–976. https://doi.org/10.2307/1353010.

Garnier, J., Billen, G., Even, S., et al., 2008. Organic matter dynamics and budgets in the turbidity maximum zone of the seine estuary (france). Estuar. Coast. Shelf S. 77, 150–162. https://doi.org/10.1016/j.ecss.2007.09.019.

Gebhardt, A.C., Schoster, F., Gaye-Haake, B., et al., 2005. The turbidity maximum zone of the yenisei river (siberia) and its impact on organic and inorganic proxies. Estuar. Coast. Shelf S. 65, 61–73. https://doi.org/10.1016/j.ecss.2005.05.007.

Groisman, P.Ya, Karl, T.R., Easterling, D.R., et al., 1999. Changes in the probability of heavy precipitation: important indicators of climatic change. Clim. Change 42, 243–283. https://doi.org/10.1023/A:1005432803188.

Herbeck, L.S., Unger, D., Krumme, U., et al., 2011. Typhoon-induced precipitation impact on nutrient and suspended matter dynamics of a tropical estuary affected by human activities in hainan, china. Estuar. Coast. Shelf S. 93, 375–388. https://doi.org/10.1016/j.ecss.2011.05.004.
Huang, Y.-G., Yang, H.-F., Wang, Y.P., et al., 2022. Swell-driven sediment resuspension in the Yangtze estuary during tropical cyclone events. Estuar. Coast. Shelf S. 267, 107765. https://doi.org/10.1016/j.ecss.2022.107765.
Jackson, R.H., Williams, P.J., le, B., Joint, I.R., 1987. Freshwater phytoplankton in the low salinity region of the river tamar estuary. Estuar. Coast. Shelf S 25, 299–311. https://doi.org/10.1016/0272-7714(87)90073-4.
Lao, Q., Lu, X., Chen, F., et al., 2023. A comparative study on source of water masses and nutrient supply in zhanjiang bay during the normal summer, rainstorm, and typhoon periods: insights from dual water isotopes. Sci. Total Environ. 903, 166853. https://doi.org/10.1016/j.scitotenv.2023.166853.
Law, C.S., Woodward, E.M.S., Ellwood, M.J., et al., 2011. Response of surface nutrient inventories and nitrogen fixation to a tropical cyclone in the southwest pacific. Limnol. Oceano 56, 1372–1385. https://doi.org/10.4319/lo.2011.56.4.1372.
Li, Y., Tang, Y., Wang, S., et al., 2023. Recent increases in tropical cyclone rapid intensification events in global offshore regions. Nat. Commun. 14, 5167. https://doi.org/10.1038/s41467-023-40605-2.
Lin, I.-I., 2012. Typhoon-induced phytoplankton blooms and primary productivity increase in the western north pacific subtropical ocean. J. Geophys. Res.: Oceans 117. https://doi.org/10.1029/2011JC007626.
Lin, J., Krom, M.D., Wang, F., et al., 2022. Simultaneous observations revealed the non-steady state effects of a tropical storm on the export of particles and inorganic nitrogen through a river-estuary continuum. J. Hydrol. 606, 127438. https://doi.org/10.1016/j.jhydrol.2022.127438.
Ling, T.-Y., Gerunsin, N., Soo, C.-L., et al., 2017. Seasonal changes and spatial variation in water quality of a large young tropical reservoir and its downstream river. J. Chem. -Ny. 2017, 8153246. https://doi.org/10.1155/2017/8153246.
Liu, Y., Tang, D., Tang, S., et al., 2020. A case study of chlorophyll a response to tropical cyclone wind pump considering kuroshio invasion and air-sea heat exchange. Sci. Total Environ. 741, 140290. https://doi.org/10.1016/j.scitotenv.2020.140290.
Lu, X., Yu, H., Ying, M., et al., 2021. Western north pacific tropical cyclone database created by the China meteorological administration. Adv. Atmos. Sci. 38, 690–699. https://doi.org/10.1007/s00376-020-0211-7.
Na, L., Na, R., Bao, Y., et al., 2021. Time-lagged correlation between soil moisture and intra-annual dynamics of vegetation on the mongolian plateau. Remote Sens 13, 1527. https://doi.org/10.3390/rs13081527.
Nilsson, G.E., Randall, D.J., 2010. Adaptations to hypoxia in fishes. In: Nilsson, G.E. (Ed.), Respiratory Physiology of Vertebrates: Life with and Without Oxygen. Cambridge University Press, Cambridge, pp. 131–173. https://doi.org/10.1017/CBO9780511845178.006.
Ploug, H., Zimmermann-Timm, H., Schweitzer, B., 2002. Microbial communities and respiration on aggregates in the elbe estuary, germany. Aquat. Microb. Ecol. 27, 241–248. https://doi.org/10.3354/ame027241.
Rhee, G., Gotham, I.J., 1981. The effect of environmental factors on phytoplankton growth: light and the interactions of light with nitrate limitation. Limnol. Oceano 26, 649–659. https://doi.org/10.4319/lo.1981.26.4.0649.
Servais, P., Garnier, J., 2006. Organic carbon and bacterial heterotrophic activity in the maximum turbidity zone of the seine estuary (france). Aquat. Sci. 68, 78–85. https://doi.org/10.1007/s00027-005-0809-y.
Tan, Q., Ge, B., Itahashi, S., et al., 2023. Unexpected high contribution of in-cloud wet scavenging to nitrogen deposition induced by pumping effect of typhoon landfall in China. Environ. Res. Commun. 5, 21005. https://doi.org/10.1088/2515-7620/acb90b.
Thompson, P.A., Paerl, H.W., Campbell, L., et al., 2023. Tropical cyclones: What are their impacts on phytoplankton ecology? J. Plankton Res. 45, 180–204. https://doi.org/10.1093/plankt/fbac062.
Wang, G., Wu, L., Mei, W., et al., 2022. Ocean currents show global intensification of weak tropical cyclones. Nature 611, 496–500. https://doi.org/10.1038/s41586-022-05326-4.
Wang, S., Toumi, R., 2021. Recent migration of tropical cyclones toward coasts. Science 371, 514–517. https://doi.org/10.1126/science.abb9038.
Wang, Y., Liu, D., Xiao, W., et al., 2021. Coastal eutrophication in China: trend, sources, and ecological effects. Harmful Algae 107, 102058. https://doi.org/10.1016/j.hal.2021.102058.
Ye, H.J., Sui, Y., Tang, D.L., et al., 2013. A subsurface chlorophyll a bloom induced by typhoon in the south China sea. J. Mar. Syst. 128, 138–145. https://doi.org/10.1016/j.jmarsys.2013.04.010.
Ying, M., Zhang, W., Yu, H., et al., 2014. An overview of the China meteorological administration tropical cyclone database. J. Atmos. Ocean. Technol. 31, 287–301. https://doi.org/10.1175/JTECH-D-12-00119.1.
Yuan, Z., Achterberg, E.P., Engel, A., et al., 2023. Phytoplankton community response to episodic wet and dry aerosol deposition in the subtropical north atlantic. Limnol. Oceano 68, 2126–2140. https://doi.org/10.1002/lno.12410.
Zhao, H., Wang, Y., 2018. Phytoplankton increases induced by tropical cyclones in the south China sea during 1998–2015. J. Geophys. Res.: Oceans 123, 2903–2920. https://doi.org/10.1002/2017JC013549.
Zhao, H., Pan, J., Han, G., et al., 2017. Effect of a fast-moving tropical storm washi on phytoplankton in the northwestern south China sea. J. Geophys. Res.: Oceans 122, 3404–3416. https://doi.org/10.1002/2016JC012286.
Zheng, G.M., Tang, D., 2007. Offshore and nearshore chlorophyll increases induced by typhoon winds and subsequent terrestrial rainwater runoff. Mar. Ecol. -Prog. Ser. 333, 61–74. https://doi.org/10.3354/meps333061.